$(O_2CC_2H_5)_2Cl_4(4\text{-Mepy})_2$ and Ph_2Ppy was refluxed in acetone, although our attempts to prepare the related PPh_3 derivative were not successful.

(a) Spectroscopic and Electrochemical Properties. The electronic absorption spectra of the five mono(carboxylato)-bridged complexes that possess the Re_2^{5+} core are very similar to one another (Table IV). The most noteworthy and diagnostic feature is the presence of an intense absorption between 1200 and 1400 nm that is assigned to the spin-allowed $\delta \rightarrow \delta^*$ transition, which is characteristic of complexes that contain the $\sigma^2\pi^4\delta^2\delta^{*1}$ electronic configuration.[1,12,13] Solutions of these complexes in CH_2Cl_2 have magnetic moments (as measured by the Evans method) that confirm the presence of one unpaired electron (e.g. for $Re_2(O_2CCH_3)Br_4(Ph_2Ppy)_2\cdot{}^1/_2(CH_3)_2CO$, $\mu_{eff} = 1.63\ \mu_B$). The paramagnetic nature of these species is further demonstrated by X-band ESR spectral measurements on $Re_2(O_2CCH_3)Cl_4(PPh_3)_2$ and $Re_2(O_2CCH_3)Cl_4(Ph_2Ppy)_2$ in CH_2Cl_2/toluene glasses at −160 °C. Both complexes show anisotropic, highly structured patterns that are centered at $g \simeq 2.16$ and 2.20, respectively, and that are located between ca. 1 and 5 kG. The spectrum of the PPh_3 complex is the best resolved, and the complexity presumably reflects hyperfine splittings arising from the rhenium ($I = {}^5/_2$) and phosphorus ($I = {}^1/_2$) nuclei. The most prominent lowest field lines in this spectrum show spacings of ca. 250 G; these are most likely assignable to the A^{Re} hyperfine splitting. The ESR spectra resemble in a general way those reported for other Re_2^{5+} species.[13-15]

The electrochemical properties of these complexes resemble one another very closely, and like other complexes that possess the Re_2^{5+} core,[1,13] they exhibit two one-electron processes, one corresponding formally to an oxidation and the other to a reduction. Consequently, the complexes $Re_2(O_2CR)X_4(PR_3)_2$ (R = Me, Et; X = Cl, Br; PR_3 = PPh_3, Ph_2Ppy) can exist in three distinct oxidation states, viz. $[Re_2(O_2CR)X_4(PR_3)_2]^{1+,0,1-}$. Voltammetric potentials as measured by cyclic voltammetry on 0.1 M TBAH/CH_2Cl_2 solutions are listed in Table IV.

(b) Crystal Structure of $Re_2(\mu\text{-}O_2CCH_3)Cl_4(PPh_3)_2$. A single-crystal X-ray structure analysis on a crystal of this complex grown from CH_2Cl_2/diethyl ether has confirmed the presence of a multiply bonded dimetal M_2L_8-type structure,[1,2] within which there is a single acetate bridging ligand. Important bond lengths and angles for this complex are listed in Table III, and an ORTEP representation of the structure is shown in Figure 1. While no crystallographic symmetry is imposed on the molecule, it possesses an essentially eclipsed rotational geometry and a surprisingly short Re–Re bond (2.216 (1) Å). This bond is significantly shorter than that found in $Re_2Cl_5(dppm)_2$ (2.263 (1) Å; dppm = $Ph_2PCH_2PPh_2$)[16] and in most quadruply bonded carboxylato-bridged dirhenium(III) complexes.[1] This shortening might be a consequence of a *single* carboxylate bridge, which can optimize the metal–metal interaction while allowing for minimization of the nonbonded repulsions between the chloride and phosphine ligands. The Re–Cl and Re–P distances and appropriate angular distortions in this molecule appear normal and reflect the essential similarity of the two metal centers in this mixed-valent species. This formulation contrasts with the valence formalism $Re^{IV}Re^{II}$ that is appropriate for the structurally characterized unsymmetrical alkoxide derivatives $(R'O)_2X_2ReReX_2(PPh_3)_2$.[4,5]

This structural study demonstrates that these molecules are the first examples of *multiply bonded* dirhenium complexes that contain a single anionic ligand bridge. The complexes $Re_2(O_2CR)X_4L_2$ have a ligand arrangement which resembles that believed to be present in $Re_2Cl_4(PMe_3)_2(\mu\text{-dppm})$ and $Re_2Cl_4(PMe_3)_2(\mu\text{-dppa})$, where dppm = $Ph_2PCH_2PPh_2$ and dppa = $Ph_2PNHPPh_2$.[17]

Since the electrochemical and spectroscopic properties of $Re_2(O_2CCH_3)X_4(PPh_3)_2$ and their Ph_2Ppy analogues are so similar, it is likely that the latter complexes have a structure closely akin to that of $Re_2(O_2CCH_3)Cl_4(PPh_3)_2$. In this event they would contain monodentate phosphorus-bound Ph_2Ppy ligands, behavior that stands in marked contrast to the previously documented tendency of this ligand to bridge multiply bonded dirhenium units.[8] Alternatively, if the Ph_2Ppy ligands are bridging (through their N, P donor sets), then two chloride ligands would presumably be axially bound.

(c) Conclusions. While alcohol solvents favor the formation of $(R'O)_2X_2ReReX_2(PPh_3)_2$ in the reactions between PPh_3 and $Re_2(O_2CCH_3)_2X_4L_2$ when L = H_2O, DMF, or Me_2SO,[4,5] the paramagnetic acetate-bridged complexes $Re_2(O_2CCH_3)X_4(PPh_3)_2$ are formed when L = py or 4-Mepy. Although the ligands L dissociate during the course of these reactions and are not incorporated into the final products, they must in some way influence the loss of the acetate ligands from $Re_2(O_2CCH_3)_2X_4L_2$. If the loss of acetate proceeds via its protonation, then L must control this step. Alternatively, the reaction course may be controlled by the lability of L, the more labile ligands (H_2O, DMF, Me_2SO)[18] favoring the alkoxide product. However, these differences may be quite subtle, since with acetone as the solvent the diaquo adducts $Re_2(O_2CCH_3)_2X_4(H_2O)_2$ react with PPh_3 to give $Re_2(O_2CR)X_4(PPh_3)_2$. We find no evidence that $(R'O)_2X_2ReReX_2(PPh_3)_2$ and $Re_2(O_2CR)X_4(PPh_3)_2$ can be converted into one another, either by the reaction of lithium acetate or acetic acid with the former or by the reaction of the latter with alcohol or with alcohol/PPh_3 mixtures.

Acknowledgment. We thank the National Science Foundation (Grant No. CHE85-06702) for research support.

Supplementary Material Available: Experimental details relating to the crystal structure determination, listings of atomic positional parameters for the phenyl ring carbon atoms (Table S1), anisotropic thermal parameters (Table S2), complete bond distances (Table S3), and complete bond angles (Table S4), and a figure showing the full atomic numbering scheme (Figure S1) (11 pages); a table of observed and calculated structure factors (17 pages). Ordering information is given on any current masthead page.

---

(12) Ebner, J. R.; Walton, R. A. *Inorg. Chim. Acta* **1975**, *14*, L45.

(13) Brant, P.; Salmon, D. J.; Walton, R. A. *J. Am. Chem. Soc.* **1978**, *100*, 4424.

(14) Brant, P.; Glicksman, H. D.; Salmon, D. J.; Walton, R. A. *Inorg. Chem.* **1978**, *17*, 3203.

(15) Srinivasan, V.; Walton, R. A. *Inorg. Chem.* **1980**, *19*, 1635.

(16) Cotton, F. A.; Shive, L. W.; Stults, B. R. *Inorg. Chem.* **1976**, *15*, 2239.

(17) Root, D. R.; Blevins, C. H.; Lichtenberger, D. L.; Sattelberger, A. P.; Walton, R. A. *J. Am. Chem. Soc.* **1986**, *108*, 953.

(18) Misailova, T. V.; Kotel'nikova, A. S.; Golovaneva, I. F.; Evstaf'eva, O. N.; Lebedev, V. G. *Russ. J. Inorg. Chem.* (*Engl. Transl.*) **1981**, *26*, 343.

Contribution from the Savannah River Laboratory,
E. I. du Pont de Nemours and Company,
Aiken, South Carolina 29808

Iron-57 Mössbauer Spectra of $MnFeF_5\cdot 2H_2O$[†]

D. G. Karraker

Received June 25, 1986

The $M^{II}M^{III}F_5\cdot 2H_2O$ compounds, where M^{II} is a divalent and M^{III} is a trivalent transition-metal ion, have the structure of "zigzag" chains of vertex-sharing $M^{III}F_6$ co-octahedra cross-linked by bridging $M^{II}F_4(H_2O)_2$ octahedra.[1] Since a variety of paramagnetic M^{II} and M^{III} ions can be substituted in this structure, compounds with interesting magnetic properties have been prepared and have been investigated by magnetic susceptibilities[1-5,8] and, when M^{II} or M^{III} is Fe^{II} or Fe^{III}, by ^{57}Fe Mössbauer spectroscopy.[2,6,7] A recent low-temperature magnetic susceptibility

---

[†] The information contained in this paper was developed during the course of work under Contract No. DE-AC09-76SR00001 with the U.S. Department of Energy.

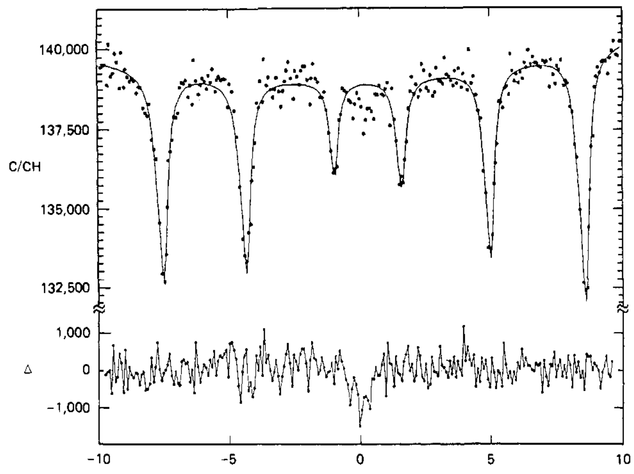

Figure 1. ^{57}Fe Mössbauer spectrum of $MnFeF_5 \cdot 2H_2O$ at 4.2 K.

study of $MnFeF_5 \cdot 2H_2O$ found a transition to ferrimagnetic ordering at 38 ± 0.25 K, in common with similar transitions for the isostructural $Fe_2F_5 \cdot 2H_2O$[3] and $CoFeF_5 \cdot 2H_2O$.[4] This paper reports an extension of these magnetic studies by Mössbauer spectroscopy in the temperature range 4.2–53 K.

Experimental Section

$MnFeF_5 \cdot 2H_2O$ samples were prepared as in the previous study by precipitation from a saturated solution at 80 °C.[1,9] The structure was verified from published X-ray diffraction patterns.[9] $MnFeF_5 \cdot 2H_2O$ is reported to be, and is, gray in natural or incandescent light but green under fluorescent light. The polycrystalline sample was pressed between two flexible layers of polyethylene to form the absorber. The density of the absorbers was about 3 mg of Fe/cm^2.

Mössbauer spectra were measured with an Austin Science Associates instrument operated in a constant-acceleration mode with both triangular and flyback waveforms. The source was 35-mCi ^{57}Co diffused into rhodium metal, and calibration was relative to the spectrum of α-iron with both source and absorber at room temperature. Calibration with an SNP standard agreed with the α-iron calibration.

Mössbauer spectra were measured in vertical transmission geometry with both source and sample at the same temperature in a Janis Veri-Temp cryostat. The sample temperature was measured with a calibrated germanium resistance thermometer and the temperature controlled by manually adjusting the heating current on flowing helium gas.

Line locations, intensities, and widths (fwhm) were determined by a least-squares computer program that assumed Lorentzian line shapes on a quadratic base line. Graphs of the difference between end data and the fitted curve were used to judge the quality of the fit. Data that were used for determination of Mössbauer parameters were taken with the triangular waveform for the motor to minimize the nonlinearity caused by vertical geometry. The halves of the data (channels 1–255, channels 256–510) were analyzed separately and the results averaged. Estimated errors of the Mössbauer parameters determined from fitted spectra are ±0.02 mm/s for δ, ±0.09 mm/s for ΔE, and ±5 kOe for H_{eff}.

The samples were collimated with a $^1/_4$-in. lead ring, which was insufficient to prevent a weak line from the stainless steel of the cryostat from affecting some spectra. The identity of this line was verified by comparison between a blank spectrum and the spectrum of a standard stainless steel absorber. This line affected the spectra either by its appearance in the difference graph or by significantly increasing the width of a line near zero velocity.

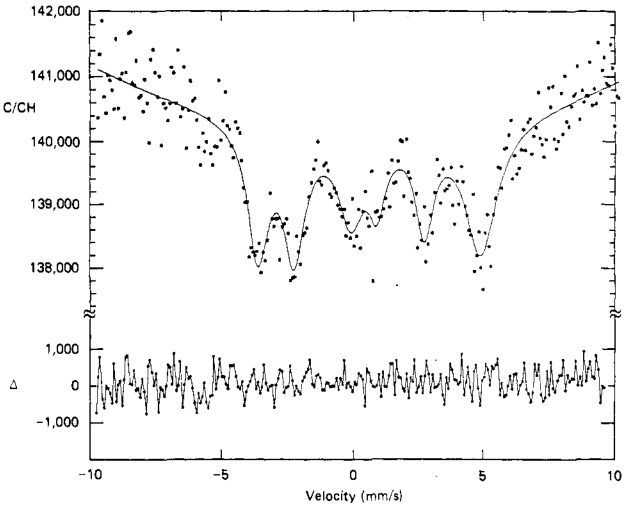

Figure 2. ^{57}Fe Mössbauer spectrum of $MnFeF_5 \cdot 2H_2O$ at 33.0 K.

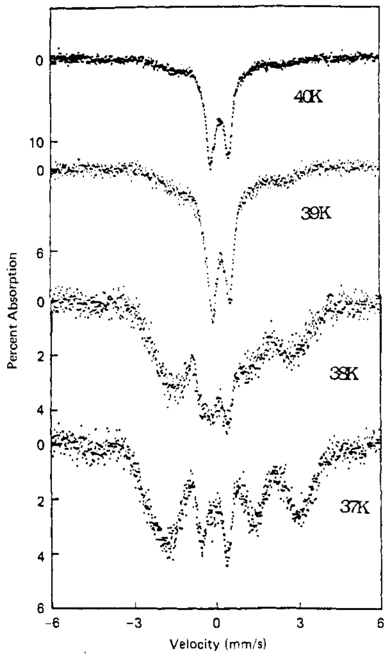

Figure 3. ^{57}Fe Mössbauer spectra of $MnFeF_5 \cdot 2H_2O$ for the anomalous region, 39–37 K.

Computer-fitted data and difference graphs are shown for $MnFeF_5 \cdot 2H_2O$ at 4.2 K (Figure 1) and at 33.0 K (Figure 2). In Figure 1 the difference graph shows the presence of the stainless steel line; in Figure 2 the stainless steel line is close enough to line 3 of the spectrum only to broaden line 3.

Results and Discussion

The ^{57}Fe Mössbauer spectra of $MnFeF_5 \cdot 2H_2O$ have three characteristic temperature regions: from 295 to ca. 40 K, the paramagnetic region; from 39 to 37 K, the so-called anomalous region; and from 35 to 4.2 K, the ordered region. The spectra from 295 to ca. 40 K show a quadrupole-split doublet with an isomer shift (δ) of 0.46 mm/s and a quadrupole coupling constant (ΔE) of 0.66 mm/s. In the anomalous region (Figure 3), between 39 and 37 K, the spectra show the change from the paramagnetic pattern to a magnetically split pattern. The ordering temperature, T_c, lies between 39 and 38 K, in agreement with the T_c determination from magnetic susceptibility measurements, 38 ± 0.25 K.[5]

Mössbauer spectra in the anomalous region between paramagnetism and complete ordering have been the subject of a number of theoretical studies that treat the change from fast to

---

(1) Hall, W.; Kim, S.; Zubieta, J.; Walton, E. G.; Brown, D. B. *Inorg. Chem.* **1977**, *16*, 1884.
(2) Walton, E. G.; Brown, D. B.; Wong, H.; Reiff, W. M. *Inorg. Chem.* **1977**, *16*, 2425.
(3) Jones, E. R., Jr.; Dawson, R. *J. Chem. Phys.* **1978**, *69*, 3289.
(4) Jones, E. R., Jr.; Dawson, R. *J. Chem. Phys.* **1979**, *70*, 2586.
(5) Jones, E. G., Jr.; Van Hine, C.; Datta, T.; Cathey, L.; Karraker, D. G. *Inorg. Chem.* **1985**, *24*, 3888.
(6) Imbert, P.; Jehanno, G.; Macheteau, Y.; Varret, F. *J. Phys.* (*Les Ulis, Fr.*) **1976**, *37*, 969.
(7) Balcerek, T. W.; Cathey, L.; Karraker, D. G. *J. Inorg. Nucl. Chem.* **1978**, *40*, 773.
(8) Jones, E. R., Jr.; Dawson, R. *J. Chem. Phys.* **1979**, *71*, 202.
(9) Gallagher, K. J.; Ottaway, M. R. *J. Chem. Soc., Dalton Trans.* **1977**, *22*, 2212.

Table I. Mössbauer Parameters for $MnFeF_5\cdot 2H_2O$

temp, K	δ, mm/s[a]	ΔE, mm/s	H_{eff}, kOe
4.2	0.43	−0.58	527
8.66	0.44	−0.58	523
13.2	0.43	−0.60	514
18.6	0.45	−0.68	485
20.1	0.41	−0.75	470
22.2	0.45	−0.74	445
26.1	0.45	−0.75	398
30.3	0.40	−0.92	325
33.0	0.40	−0.99	276
35.0	0.44	−1.11	207
37.0		~0	180 ± 20[b]
39.4	0.46	0.61	
40.5	0.48	0.69	
53	0.47	0.66	
RT	0.46	0.64	

[a] Relative to α-iron. [b] Estimated.

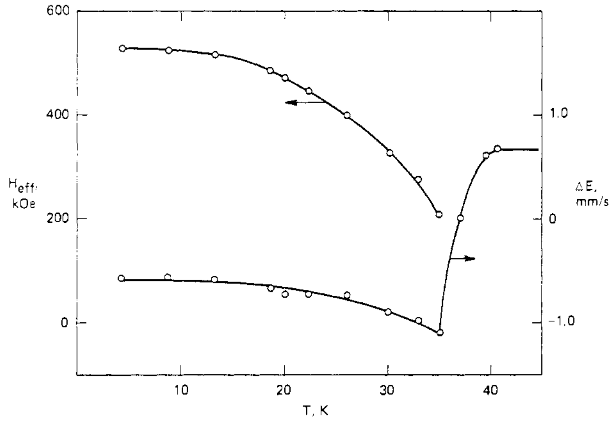

Figure 4. Mössbauer parameters for $MnFeF_5\cdot 2H_2O$ vs temperature.

slow relaxation.[10-13] The model that qualitatively fits these spectra best is that of Hoy and Corson.[14] Their model considers an insulator just above T_c as composed of paramagnetic regions and clusters of spins with small values of reduced magnetization. The spins in paramagnetic regions are fluctuating rapidly, and the spins of the cluster regions fluctuating more slowly. As the temperature is lowered, the relative amount of paramagnetic to spin clusters decreases until the paramagnetic component disappears (ca. 37 K for $MnFeF_5\cdot 2H_2O$) and is replaced by an ordered region with significant values of reduced magnetization. This ordered component increases relative to the spin clusters until at lower temperatures only the ordered component is shown by the spectrum (Figure 2).

The data for the ordered region are shown in Table I and Figure 4. The effective internal field, H_{eff}, increases smoothly with decreasing temperature to reach a value of 527 kOe at 4.2 K. The quadrupole-splitting constant, ΔE, is −0.58 at 4.2 K and slowly decreases to −1.1 at 35 K. Between 35.0 and 39.4 K, there is a virtual discontinuity as ΔE increases to its paramagnetic value of 0.65 mm/s as paramagnetism replaces ordering.

The H_{eff} values for the Fe^{3+} Mössbauer parameters of $MnFeF_5\cdot 2H_2O$ are in excellent agreement with the Fe^{3+} Mössbauer parameters for $Fe_2F_5\cdot 2H_2O$ determined by Walton et al.[2] and Imbert et al.[6] At 4.2 K, the H_{eff} of 527 kOe for $MnFeF_5\cdot 2H_2O$ may be compared with H_{eff} of 532 kOe[2] and 538 kOe[6] determined for $Fe_2F_5\cdot 2H_2O$. At 20 K, the H_{eff} of 460 kOe[2] for $Fe_2F_5\cdot 2H_2O$ may be compared with 470 kOe determined for $MnFeF_5\cdot 2H_2O$ in this study. The Mössbauer parameters for $MnFeF_5\cdot 2H_2O$ do not show the transition below T_c found by Imbert et al.[6] on a sample of $Fe_2F_5\cdot 2H_2O$ prepared by dehydration of $Fe_2F_5\cdot 7H_2O$. Walton et al.[2] did not observe this transition on crystalline $Fe_2F_5\cdot 2H_2O$. The $MnFeF_5\cdot 2H_2O$ samples in this work were prepared by the same procedure as that used by Walton et al.

The quadrupole-splitting constant of 0.65 mm/s for Fe^{3+} in $MnFeF_5\cdot 2H_2O$ is essentially the same in the paramagnetic region of the spectrum as those reported for Fe^{3+} in $Fe_2F_5\cdot 2H_2O$, 0.65 and 0.59 mm/s.[2,6,7] However, the ΔE for $MnFeF_5\cdot 2H_2O$ in the ordered region is a factor of 6 greater than the ΔE of −0.105 mm/s found by Imbert et al.[6] for $Fe_2F_5\cdot 2H_2O$ in the same region. Presumably, this reflects the stronger crystal field from the Mn^{2+} ($3d^5$) ion than from the Fe^{2+} ($3d^4$) ion.

In general, this study shows the Fe^{3+} ion in $MnFeF_5\cdot 2H_2O$ to have magnetic properties very similar to those of Fe^{3+} in $Fe_2F_5\cdot 2H_2O$. This result might clarify the problem of the saturation magnetization of $MnFeF_5\cdot 2H_2O$.[5] The saturation magnetization of $Fe_2F_5\cdot 2H_2O$ agrees nicely with a simple model for negative exchange, $\mu(Fe^{3+}) - \mu(Fe^{2+}) = 1.0\ \mu_B$ vs the experimental 1.2 μ_B.[2] Substitution of Mn^{2+} for Fe^{2+} by the same model would lead to $\mu_B = 0$, rather than 1.1 μ_B found by Jones et al.[5] The determination of this work that the Fe^{3+} ions in $MnFeF_5\cdot 2H_2O$ and $Fe_2F_5\cdot 2H_2O$ have very similar magnetic properties suggests that the agreement found for the simple model of negative exchange may be fortuitous; and a more complicated model, involving magnetic sublattices, may be required to be consistent with both compounds.[15] The explanation for the differences in the T_c temperatures for $MnFeF_5\cdot 2H_2O$ and $Fe_2F_5\cdot 2H_2O$ may also lie with such a model.

Registry No. $MnFeF_5\cdot 2H_2O$, 66106-43-2.

---

(10) Wickham, H. H.; Wertheim, G. K. In *Chemical Applications of Mössbauer Spectroscopy*; Goldanski, V. I., Herber, R. H., Eds.; Academic: New York, 1968.

(11) Clauser, M. J.; Blume, M. *Phys. Rev. B: Solid State* **1971**, *3*, 583.

(12) Dattagupta, S.; Blume, M. *Phys. Rev. B: Solid State* **1974**, *10*, 4540.

(13) Jones, D. H.; Srivastava, K. K. P. *Phys. Rev.* **1968**, *34*, 7542.

(14) Hoy, G. R.; Corson, M. R. In *Mössbauer Spectroscopy and Its Chemical Applications*; Stevens, J. G., Shenoy, G. K., Eds.; Advances in Chemistry 194; American Chemical Society: Washington, DC, 1981; pp 463–479.

(15) Smart, J. S. *Effective Field Theories of Magnetism*; W. B. Saunders: Philadelphia, PA, 1966.

Contribution from the Savannah River Laboratory,
E. I. du Pont de Nemours and Company,
Aiken, South Carolina 29808

Iodine-129 Mössbauer Study of Actinide Iodides[†]

D. G. Karraker

Received November 26, 1986

The ^{129}I Mössbauer effect can provide information on the bonding characteristics of iodine-containing compounds. Previous studies[1,2] investigated LaI_3, GdI_3, and ErI_3 and found a slight effect on the 5p electron distribution in these compounds. Four actinide iodides, ThI_4, UI_4, NpI_3, and PuI_3, were investigated in this study to compare with the lanthanide iodides.

Experimental Section

The compounds were prepared from ^{129}I obtained as an $Na^{129}I$ solution from the Isotopes Division of Oak Ridge National Laboratory (ORNL). $Hg^{129}I_2$ was precipitated from solution, centrifuged, washed, and dried under vacuum for 2–3 days. Actinide iodides were prepared by reacting actinide metals with a 20% excess of $Hg^{129}I_2$ at 350–400 °C in evacuated, sealed glass tubes.[3] Typical preparations used 20–30 mg of the actinide metal and 80–90 mg of $Hg^{129}I_2$.

The source for the Mössbauer study was an $Mg_3{}^{129}TeO_6$ pellet, prepared from enriched ^{128}Te by the Isotopes Division of ORNL and irradiated for 2 weeks in the ORNL HIFR reactor.[4] Samples contained about 20 mg of the compound under study sealed between two layers of plastic.

[†] The information contained in this paper was developed during the course of work under Contract No. DE-AC09-76SR00001 with the U.S. Department of Energy.

0020-1669/87/1326-3816$01.50/0 © 1987 American Chemical Society